

# Effect of Oxalic Acid in the Self-Assembled Structure of Sodium Carboxymethyl Cellulose

Rohit Omar\* and Rahul Omar

Department of Cement Technology

AKS University, Satna-485001

Madhya Pradesh, India

\*Corresponding author

Mob: +91-8887825529; Email address: [omariitd@gmail.com](mailto:omariitd@gmail.com)

## Abstract:

Evaporation of sessile droplets containing Sodium Carboxymethyl Cellulose induces outward flow within the drop, which is commonly well known as “coffee ring” effect or a dense ring like deposition along the perimeter. In this work, the formation of self-assembled structure during drying of microliter drops containing Sodium Carboxymethyl Cellulose with oxalic acid is investigated with the help of optical microscope. The structure formation is also influenced by evaporative flux and Marangoni flow inside the liquid drop. The different parameters such as sodium carboxymethyl cellulose concentration, acid concentration, drying time, drying temperature, humidity, stirring velocity, stirring temperature, pH and drop volume strongly influences the structure formation.

**Keywords:** Self-assembly, Sodium Carboxymethyl Cellulose, Coffee-ring effect, Sessile drop, Fractal dimension, Box-counting method

## 1. Introduction

Self-assembly refers to the process by which nanoparticles or other discrete components spontaneously organize due to specific interactions, through their environment. Self-assembly is typically associated with thermodynamic equilibrium, the organized structures being characterized by a minimum in the system's free energy. Essential in self-assembly is that the building blocks organize into ordered,

macroscopic structures, either through direct interactions (*e.g.*, by interparticle forces), or indirectly using a template or an external field.

Self-assembly is the force balance process between three classes of forces: attractive driving, repulsive opposition and directional force. Directional force can be considered functional force in the sense that it is also responsible for functionality. When only the first two classes of forces are in action, the self-assembly process is a random and usually one-step process. Self-assembly is the fundamental principle which generates structural organization on all scales from molecules to galaxies. It is defined as reversible processes in which pre-existing parts or disordered components of a pre-existing system form structures of patterns.

Self-assembly typically employs asymmetric molecules that are pre-programmed to organize into well-defined supramolecular assemblies. Most common are amphiphilic surfactant molecules or polymers composed of hydrophobic and hydrophilic parts. The main driving force to self-assembled monolayers is the strong chemical bond of building units with the solid substrates and the intermolecular forces between the building units.

Self-assembly has a fundamental advantage over mechanically directed assembly: It requires no machinery to move and orient components, letting random, Brownian motion do the job instead. Selective binding between uniquely matching surfaces compensates for the randomness of the motions that bring components together. Molecular synthesis methods and self-assembly can be used to produce automatically precise nano systems. The disadvantage of pure self-assembly is that for every product, the structure of the parts must encode the structure of the whole. This requires that components be more complex, which tends to make design and fabrication more difficult.

Self-assembly formation of nano or colloidal particles can be broadly classified into dry methods<sup>1,2,3</sup> and liquid phase methods<sup>4,5</sup>. Formation in dry condition include chemical vapor deposition, laser ablation etc. Liquid phase formation of self-assembly can again be classified into (1) inside the bulk media and (2) onto the solid surface. Self-assembly onto the solid surface may occur because of the adsorption of the particles on the surface<sup>6,7</sup> or during the evaporation of a liquid drop.<sup>8,9</sup>

Evaporation of liquid drops containing nanospheres resulted in circular deposition patterns. The circularity of the patterns depended on the uniformity of the surface tension on the substrate. By employing binary suspensions, containing two differently sized nanospheres, it was possible to modulate the fine structure of such rings. Slow evaporation on mirror-polished substrates resulted in well-ordered distributions, where larger particles self-assembled in dense hexagonal packages, forming apparently an external ring, deposited around the massive inner ring. Deposition started at the air/liquid/solid-contact line. Results could inspire principles for the fabrication of optical devices and may be fruitfully used to design biomaterials with cell-selective properties.<sup>10,11</sup>

A simple model is employed to predict the radial arrangement of nanospheres in rings. Deviations from a standard order (predicted by the model) may be useful to detect biologically active nanoparticles.

Ring formation has been described for various nanoparticles: silver, copper, cobalt, cadmium sulfide, barium ferrite, and gold.<sup>12,13</sup> The mechanism of formation has been explained in terms of the interaction between wetting properties, capillary forces, surface tension, and evaporation-driven convective flows resulting from temperature gradient. However, for nanoparticles suspended in liquid drops, gravity is likely to considerably affect both dynamics (rate of sedimentation) and pattern formation in the rings.<sup>14,15</sup>

A relatively simple approach to deposit particles onto a substrate is by evaporation of a colloidal dispersion droplet. In droplets with pinned contact lines, evaporation gives rise to the so-called coffee-stain effect.<sup>16,17</sup> In an evaporating drop with an immobile contact line, a capillary flow is generated to replenish the liquid that has evaporated from the edges. This flow drags particles towards the contact line, forming the ring-shaped stain in particle suspensions such as coffee.<sup>18,19</sup>

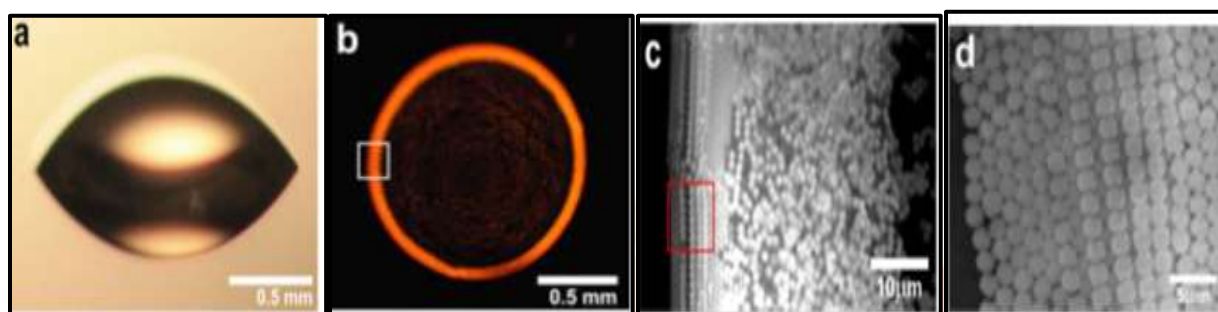


**Figure 1** Order-to-disorder transition in the particle stain left by an evaporating drop.

When the droplet has completely evaporated, most of the colloidal particles have aggregated into a ring-shaped coffee stain Fig. 1 (b). Zooming in on the stain, we see that the particle arrangement is not homogeneous as shown in Fig. 1 (c); there is a remarkable transition from a crystalline arrangement to a disordered phase. A top view of the stain, Fig. 1 (d) shows a sequence of particle arrangements within the ordered phase, starting from hexagonal packing, followed by square packing, and again hexagonal packing.<sup>20,21,22</sup>

The self-assembly of colloidal particles can be carried out using virtually any particle ranging from SiO<sub>2</sub> particles, polymer particles, glass particles or even particles synthesized in the reaction media where the particle solution is directly used for self-assembly purposes and on any substrate for that matter.<sup>23,24,25</sup> The structure formed at the edge of drop is depends heavily on the interaction between the particle, the substrate and the carrier fluid of the particles. The work which pioneered the whole race of self-assembly using colloidal particles was by Deegan et al., 1997. In their experiments ring like patterns formed from dried liquid drops, now famously called “coffee ring” effect.

Nanostructured surfaces are prepared primarily by two techniques: Lithography and self-assembly. Out of these two techniques, self-assembly is simple and less cost effective. Self-assembly result from evolution of a system based on kinetic and thermodynamic considerations. The formation of self-assembled structure results due to crystal growth.<sup>26,27</sup> In crystal growth, periodic arrangement of atoms results from

the energy and entropy considerations. Another interested example of self-assembly is thin film growth. In thin film growth from the vapor phase, atoms are adsorbed on the surface, subsequent an atom diffusion and relevant interaction to the substrate.<sup>28,29</sup>

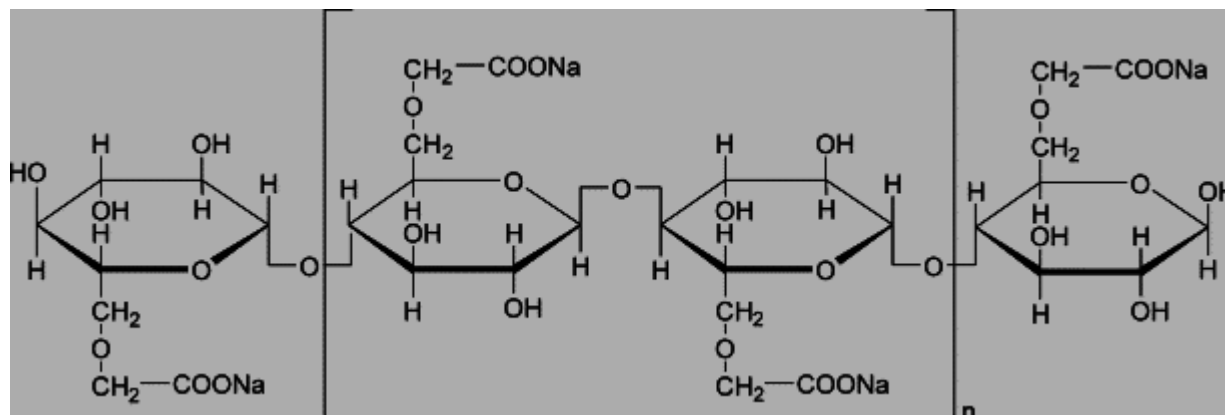


**Figure 2 Structure of Sodium Carboxymethyl Cellulose**

The term polyelectrolyte is meant a high molecular weight substance that is simultaneously also an electrolyte containing a number of ionizable groups distributed along the polymer chain. Carboxymethyl cellulose is a cellulose derivative with carboxymethyl groups (-CH<sub>2</sub>-COOH) bound to some of the hydroxyl groups of the glucopyranose monomers that make up the cellulose backbone. In other words, it is a compound of cellulose in which some of the cellulose -OH groups have been converted into a structure of the type -O-CH<sub>2</sub>-COOH. The polyelectrolytes dissociate into a macro ion and counter ions in aqueous solution.

One typical feature of the polyelectrolytes is the extremely low activity coefficient of the counter ion. If the charge density of polyelectrolyte is high enough, a fraction of counter ions is located in the vicinity or at the surface of macro ion (condensed fraction of counter ions). The physical background of the counter ion-condensation effect is the competition between a gain in energy in the electrostatic interaction and a loss of entropy in the free energy. Another interesting feature of the polyelectrolytes is the high expansion or 'stretching' of the poly ion chain due to strong electrostatic repulsion between charged segments.

## 2. Materials and Method

The chemicals used in this experiment were procured from the following companies, Sodium Carboxymethyl Cellulose [C<sub>6</sub>H<sub>7</sub>O<sub>2</sub>(OH)<sub>x</sub>(OCH<sub>2</sub>COONa)<sub>y</sub>]<sub>n</sub> 99% purity from Loba chemicals (India), and Oxalic acid (H<sub>2</sub>C<sub>2</sub>O<sub>4</sub>·2H<sub>2</sub>O) 99% purity from Merck (India). All chemicals were used as received without any further purification. Ultrapure water having resistivity of 18 MΩ cm and pH 6.4–6.5 was used for all the experiments.

Sodium Carboxymethyl Cellulose in aqueous media was prepared from the stock solution of higher concentration with different acids. The proper mixing of cellulose and acids proceed by magnetic stirrer

with continuous stirring at 600 rpm maintaining the temperature at 30°C about 20 minutes. The glass slides were initially washed with alcohol and then deionized water, and dried in a hot air oven. Then the solution was dropped onto the glass slide using a microliter syringe (Hamilton) with different drop volumes (1 $\mu$ l to 10 $\mu$ l) to study the drop volume also. Then the slides containing droplets were dried in a hot air oven at 30°C for more than 210 minutes with a constant relative humidity of 30%. The resulting dried drops were observed under an optical microscope (Hund, D600).

### 3. Results and Discussion

#### 3.1 Effect of Oxalic acid concentration with 0.1 wt.% Sodium Carboxymethyl Cellulose

Self-assembled structures of cellulose on hydrophilic glass surface after drying of small drops were studied using an optical microscope. The structures presented here are definitely an example of dendritic crystallization due to the presence of the crystallizable sodium oxalate salt and the cellulose molecules. Hence, the structures formed here also follow a natural fractal pattern but under the influence of the coffee-ring effect and Marangoni flows. This lends uniqueness to the fractal patterns, apart from the basic structure the branches would follow depending on the unit cell of the salt crystal. Now in the present study, it is evident that the structures tend to grow from the perimeter towards the center of the drop and the structures seem too organized and well formed to be simply attributed to diffusion limited aggregation (DLA).

Fractal tree like pattern formation is not strictly self-similar as that of mathematical defined fractals such as Kohn curve and Sierpinski's hexagonal gasket. At 0.1 wt.% cellulose with 5 mM Oxalic acid, the self-assembled tree like structure tends to grow from the periphery of the drop and central region of the drop almost empty Figure 3 (a). The magnified image of the drop clearly depicts the fact that branches tend to grow continuously from the stem with fractal pattern Figure 3 (b).

The plausible explanation may be due to the evaporative flux; initially molecules are moved towards the periphery of the drop and within the thin film of the liquid they experience an attractive force. Once the molecules are close enough because of this attractive capillary force, Van der Waals force also helps them to get attached to each other, as a result they arrange in systematic manner to form the self-assembly. Initially the majority of precursors move and deposit at the drop periphery and generate a large diameter base of the stem. Then latter the smaller molecules attach on these large diameter stems and gradually a thinner stem grows towards the center forming a finer structure.

At low acid concentration (5 mM) with 0.1 wt.% cellulose, the central region does not have any structure due to mobility of the molecules increase at the periphery of drop. However, increasing the acid concentration (20 mM) with constant sodium carboxymethyl cellulose concentration, the structure becomes dense Figure 3 (d). Since the molecules can easily agglomerate due to Ostwald ripening. This is a spontaneous process that occurs because larger crystals are more energetically favored than smaller crystals while the formation of many small crystals is kinetically favored, (i.e. they nucleate more easily) large

crystals are thermodynamically favored. Thus, from a standpoint of kinetics, it is easier to nucleate many small crystals. However, small crystals have a larger surface area to volume ratio than large crystals. Molecules on the surface are energetically less stable than the ones already well ordered and packed in the interior. Large crystals, with their greater volume to surface area ratio, represent a lower energy state. Thus, many small crystals will attain a lower energy state if transformed into large crystals.

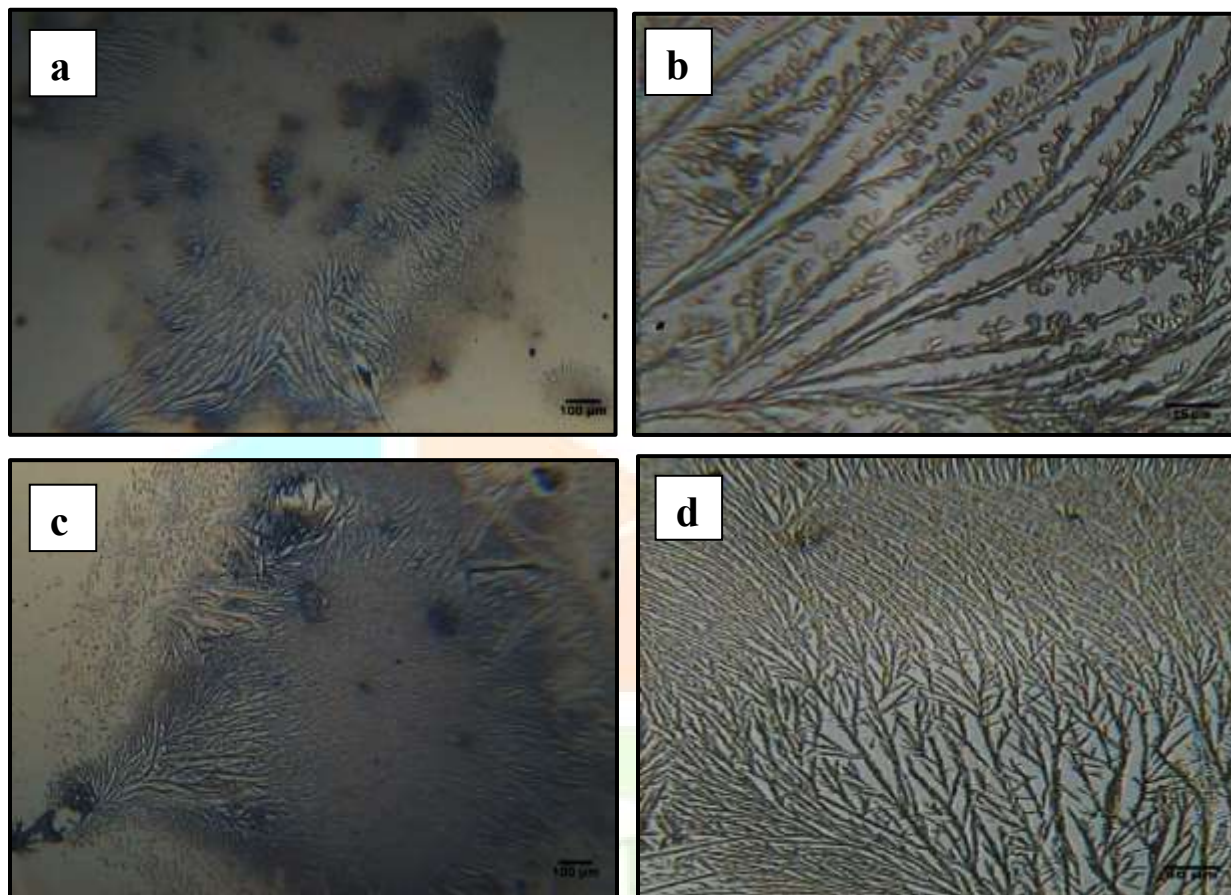


**Figure 3** Self-assembled structure of Sodium Carboxymethyl Cellulose with 0.1 wt.% in the presence of 5 mM Oxalic acid (a, b) and 20 mM Oxalic acid (c, d).

The formation of fractal tree like pattern at the periphery of the drop is to be supported by fractal dimension, which is analyzed by Fractal Analysis Software (Sasaki et al., 1994). Fractal dimension is the main tool used to describe the fractal geometry and the heterogeneity of irregular shapes. It allows capturing what is lost in traditional geometrical representations of shapes.

For a fractal curve that lies completely within two dimensional plane, the fractal dimension is greater than one (the Euclidean dimension of curve). The closer fractal dimension is to one, the smoother the fractal curve. If fractal dimension becomes two, we have Peano curve that is the curve completely fills a finite region of two dimensional spaces. The fractal dimensions of these two curves at lower and higher magnification are 1.8084 and 1.8178 respectively with correlation coefficient of 0.99. On the other hand, fractal dimension of the curves at higher acid concentration with 0.1 wt.% sodium carboxymethyl cellulose

increases which corresponds to 1.8244 and 1.8522 as well as coverage percentage or difference of brightness increases.

This fractal dimension value gives a quantitative measure of the self-similarity of the structures and their increasing complexity with length scale. This demonstrates that higher acid concentration with constant cellulose concentration the structure becomes less fractal as well as dense. It should be noted that there is a linear relationship between coverage percentage and fractal dimension and if lower the fractal dimension, it attains smoothness. The table 1 also depicts that item of coverage changes the difference of brightness depending on the image. Fractal dimension of cellulose fractal “trees” and their shapes likely indicate that these fractal “trees” are formed via diffusion limited aggregation (DLA) process.

**Table 1:** Fractal Analysis of images of 0.1 wt.% sodium carboxymethyl cellulose with 5 mM Oxalic acid (a, b) and 20 mM Oxalic acid (c, d)

Image no.	Width, height	Coverage (%)	Correlation coefficient	No. of data to calculate	Fractal Dimension
a	640, 480	38.6	0.9985	8	1.8084
b	640, 480	40.1	0.9984	8	1.8178
c	640, 480	41.1	0.9987	8	1.8244
d	640, 480	44.3	0.9985	8	1.8522

The graph between  $\log_{10}(\text{box size}) - \log_{10}(\text{count})$  are also displayed whether to check the image is fractal or not by linearity with Fractal Analysis Software. The box-counting method provides the grids with a varying number of boxes are superimposed on an image of the pattern of interest. If a structure is fractal (i.e., self-similar over multiple scales of dimension), the log of the number of boxes that are filled plotted against the log of the total number of boxes yields a straight line.

It is proposed to assign the smallest number of boxes to cover the entire image surface at each selected scale as required, thereby yielding more accurate estimates. Fractal pattern introduces spaces of a range of sizes. Thus, there is hierarchy of space sizes including few large and many small spaces. On the other hand if the spaces are all about the same size with tightly packed, there is no hierarchy of structure that characterizes fractals. The inset of box counting is to quantify fractal scaling but from a practical perspective this would require the scaling be known. In fractal analysis, however, the scaling factor is not always known ahead of time, so box counting algorithms attempt to find an optimized way of cutting a pattern up that will reveal the scaling factor.

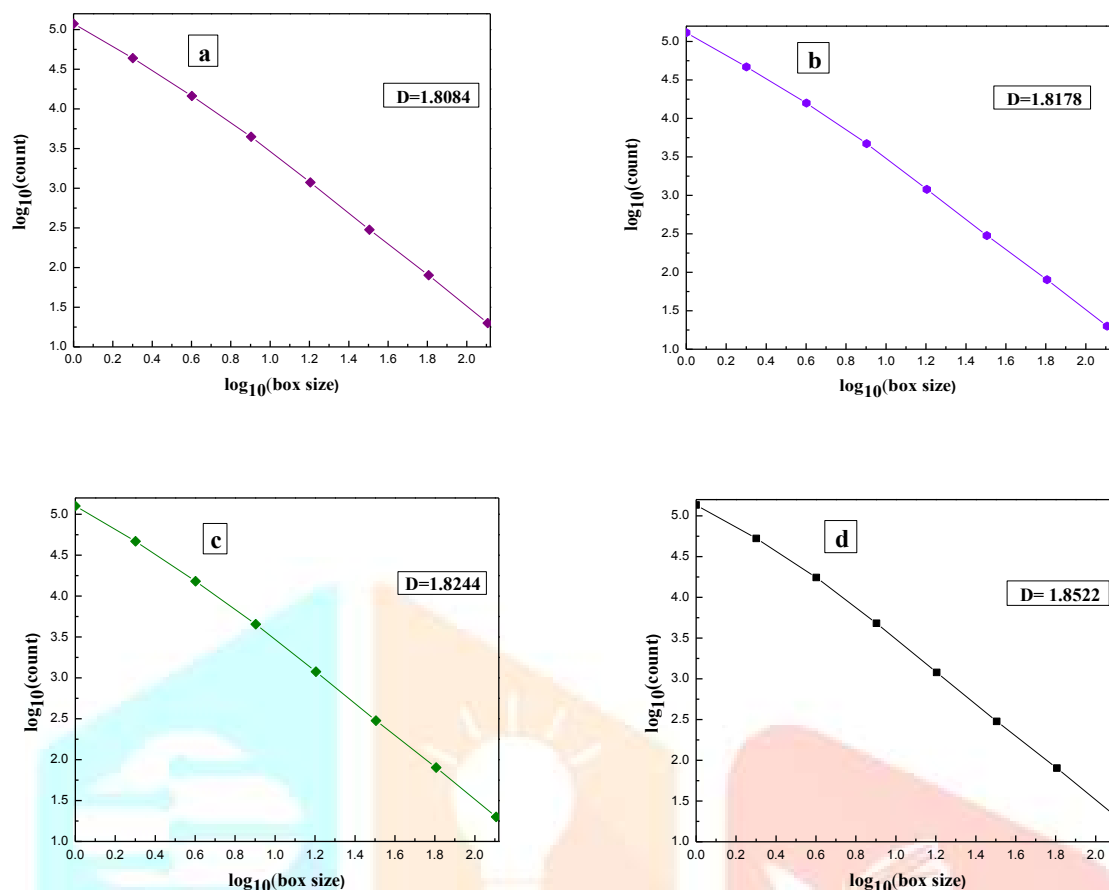


**Figure 4**  $\log_{10}(\text{box size}) - \log_{10}(\text{count})$  plot for 0.1 wt.% sodium carboxymethyl cellulose with 5 mM Oxalic acid (a, b) and 20 mM Oxalic acid (c, d) at different magnifications.

The graphs typically depict that increasing the box size, count data rapidly decline. This demonstration reveals the fact that there is hierarchy of space sizes with few large and many small spaces, as a result there is a linear relationship between  $\log_{10}(\text{box size})$  vs.  $\log_{10}(\text{count})$  with correlation coefficient of 0.9971 and 0.9972 respectively that characterize the fractal “tree” pattern.

### 3.2 Effect of oxalic acid concentration with 0.2 wt.% Sodium Carboxymethyl Cellulose

It is observed that increasing the sodium carboxymethyl cellulose concentration with 5 mM Oxalic acid, the structure tends to grow from the periphery of the drop and fractal pattern with separating blocks are observed in the central region Figure 5 (a, b). This demonstrates that only unstable growth and coarsening steps are proceed at low concentration of Sodium Carboxymethyl cellulose in the pattern formation. The driving force for this scale coarsening is the reduction of the excess free energy associated with the interface between different phases. The interface density  $S_v = S / V$ , i.e. the interface area  $S$  per unit volume  $V$ , decreases with time and therefore the characteristic size scale of the interface system given by  $1 / S_v$  increases, the microstructure coarsens. Fragmentation stage has attained with increasing the cellulose concentration (0.2 wt.%) at low acid concentration and finally reached to equilibrium condition. SEM



images of 0.2 wt.% sodium carboxymethyl cellulose with 5 mM acid concentration are shown in figure 5 (e, f). However, increasing the acid concentration, the structure tends to grow from the periphery of the drop with tree like ramified structure and finally dense structure has attained in the central region as shown in figure 5 (c, d).

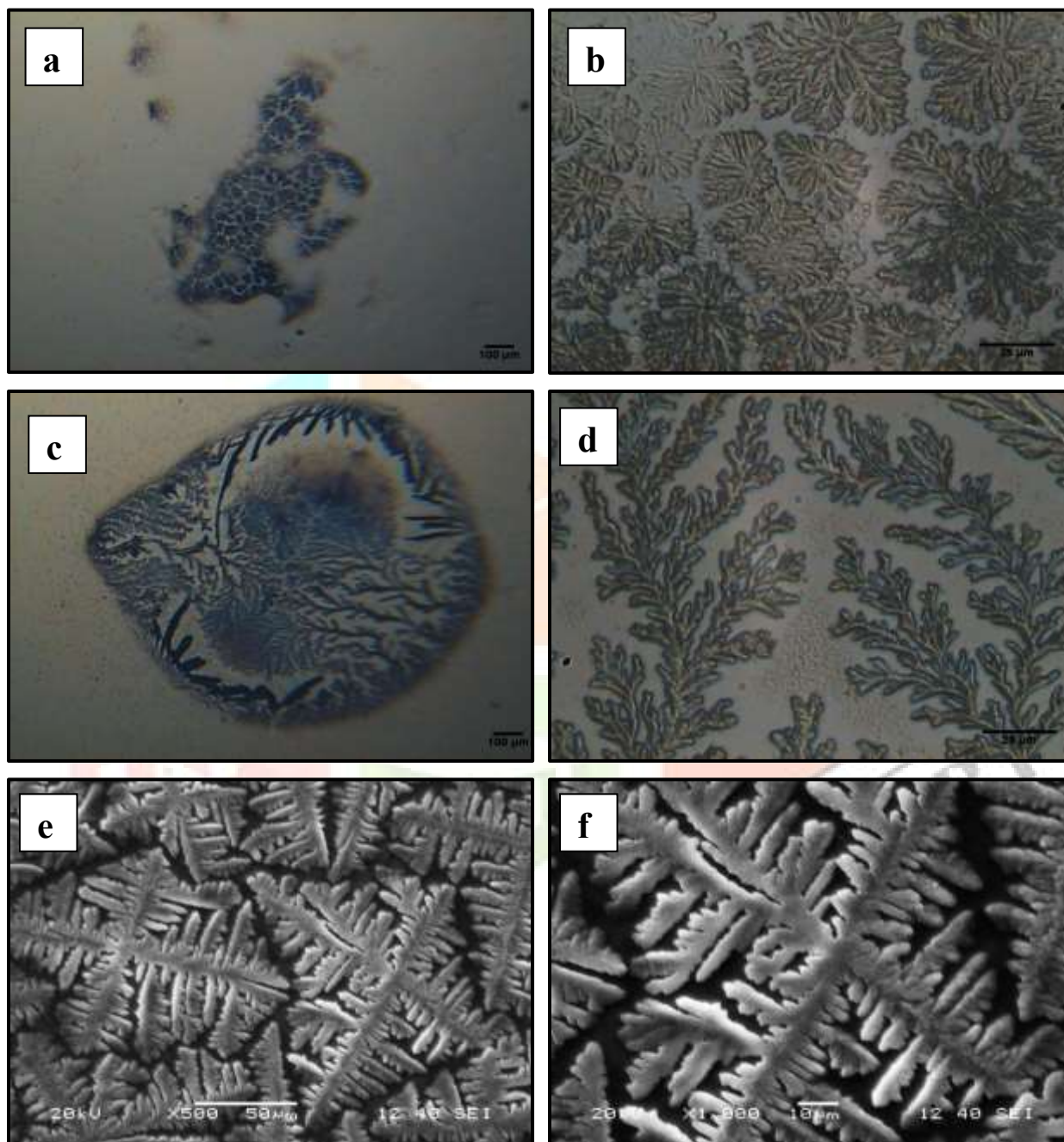


**Figure 5** Self-assembled structure of Sodium Carboxymethyl Cellulose with 0.2 wt.% in the presence of 5 mM Oxalic acid (a, b), SEM images (e, f) and 20 mM Oxalic acid (c, d).

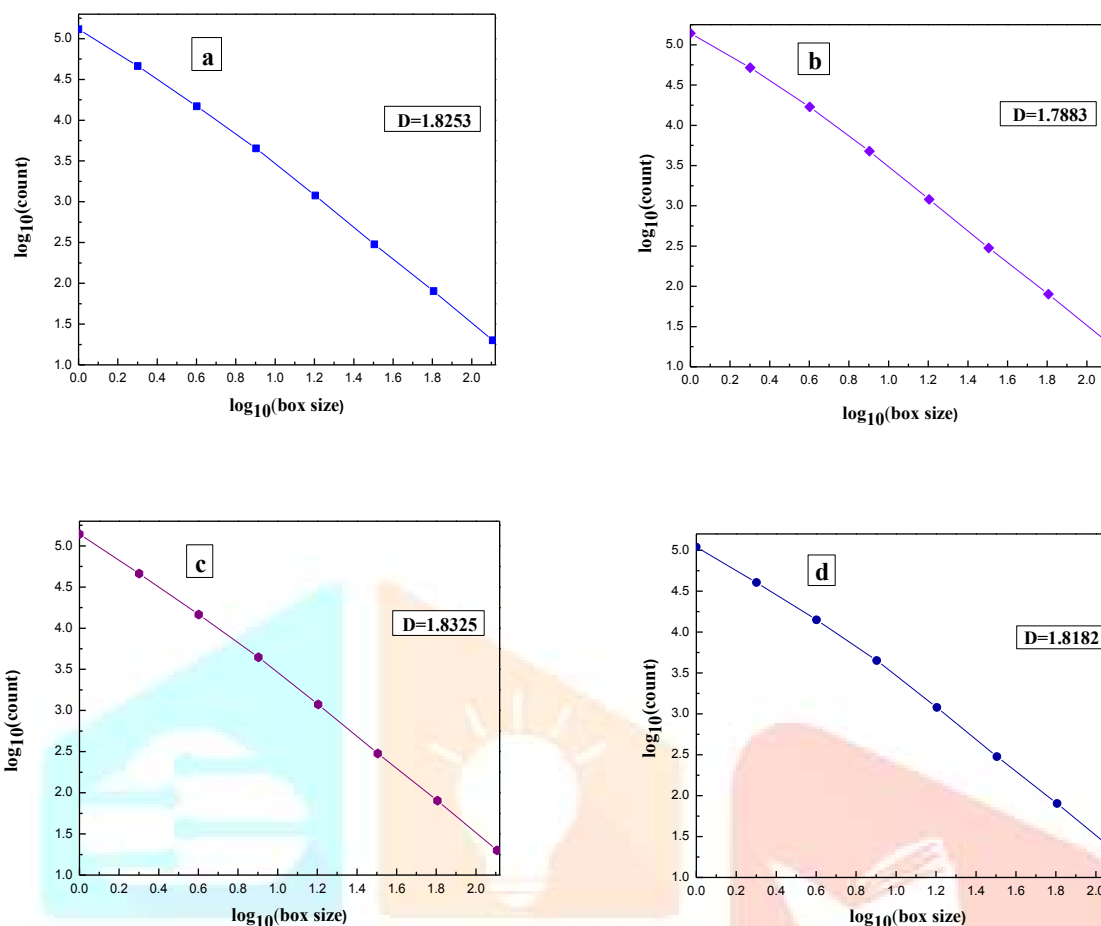


**Figure 6**  $\log_{10}(\text{box size}) - \log_{10}(\text{count})$  plot for 0.2 wt.% sodium carboxymethyl cellulose with 5 mM Oxalic acid (a, b) and 20 mM Oxalic acid (c, d) at different magnifications.

### 3.3 Effect of pH in the self-assembled structure of Sodium Carboxymethyl Cellulose in the presence of Oxalic Acid

Fractal character of the pattern gradually increases with increasing pH, when pH increased from 3.5 to 5.3. This is due to the COONa groups on sodium carboxymethyl cellulose become deprotonated with increasing pH. As a result, the energy barrier between two neighboring branches increases and screening effect becomes strong. Screening effect arises due to the fact that the inner electron are more attracted towards the nucleus so that the inner electron will not allow the nuclear charge to pass through as a result the outer electron will get a lower nuclear charge than the inner electron. Consequently fractal trees were not obtained at lower pH values.

At low pH value, cellulose molecules adhered to each other and structure becomes dense in the formation of fractal tree like pattern. This is because the charge repulsion force between two neighboring molecules decrease due to the protonation of COONa group at lower pH value. Besides the protonation effect, sodium oxalate salt also plays a crucial role in the formation of structure. Fractal dimension is another parameter to clarify the structure. It is observed from the fractal analysis that higher fractal “tree”

like ramified structure with equilibrium conditions are accompanied with low fractal dimension value at higher pH. The item of coverage also changes the difference of brightness for different images as shown in Figure 7.



**Figure 7** Effect of pH in the self-assembled structure of Sodium Carboxymethyl cellulose (a) pH=3.5, (b) pH=4.0, (c) pH=4.5, (d) pH=5.3.

#### 4. Conclusions

The structure is formed during the evaporation of liquid drop on solid surface due to crystallization of respective salt, the interplay of evaporative liquid flux and Marangoni flow inside the drop, capillary and van der Waals attractive forces. The fragmented fractal “tree” like pattern of sodium carboxymethyl cellulose is observed with oxalic acid. Some parameters are very important such as sodium carboxymethyl cellulose concentration, acid concentration, drying time, drying temperature, humidity, stirring velocity, stirring temperature, pH and drop volume for the formation of self-assembled structure.

The fine structure is generated at low acid concentration while the sodium carboxymethyl cellulose concentration depends on the type of organic acid (monobasic, dibasic or tribasic). Fractal characters of the pattern gradually disappear with decreasing pH. Fractal dimensions of these fractal patterns are in the range of 1.77 – 1.85 which follow the diffusion limited aggregation (DLA) mechanism. The box size vs. count plots on the logarithmic scale provides the linearity; as a result follow the fractal pattern.

#### References

1. Bai, F.; Zeng, C.; Yang, S.; Zhang, Y.; He, Y.; Jin, J. “The formation of a novel supramolecular structure by amyloid of poly-L-glutamic acid”, *J. Biochem. Biophys. Res. Commun.* (2008), 369, 830–834.
2. Banerjee, R.; Hazra, S.; Banerjee, S.; Sanyal, M. K. “Nanopattern formation in self-assembled monolayers of thiol-capped Au nanocrystals”, *Phys. Rev. E* (2009), 80, 056204.
3. Brune, H.; Romainczyk, C.; Roder, H.; Kern K. “Mechanism of the transition from fractal to dendritic growth of surface aggregates”, *Nature* (1994), 369, 9, 469-471.
4. Cai, Y.; Newby, Bi-min Z. “Marangoni Flow-Induced Self-Assembly of Hexagonal and Stripelike Nanoparticle Patterns”, *J. Am. Chem. Soc.* (2008) 130, 6076–6077.

5. Chiu, C.-Wei; Lee, T.-Chien; Hong, P.-Da; Lin, J.-Jen “Controlled self-assemblies of clay silicate platelets by organic salt modifier” *J. Royal Society of Chemistry* (2012), 2, 8410–8415.
6. Chon, C. H.; Paik, S.; Jr., J. B. T.; Kihm, K. D. “Effect of Nanoparticle Sizes and Number Densities on the Evaporation and Dryout Characteristics for Strongly Pinned Nanofluid Droplets”, *Langmuir* (2007), 23, 2953-2960.
7. Dai, L. L.; Sharma, R.; Wu C. Y. “Self-Assembled Structure of Nanoparticles at a Liquid-Liquid Interface”, *Langmuir* (2005), 21, 2641-2643.
8. Deegan, R. D.; Bakajin, O.; Dupont, T. F.; Huber, G.; Nagel, S. R.; Witten, T. A. “Capillary flow as the cause of ring stains from dried liquid drops”, *Nature* (1997), 389, 827-829.
9. Girard, F. ; Antoni, M.; Sefiane, K. “On the Effect of Marangoni Flow on Evaporation Rates of Heated Water Drops”, *Langmuir* (2008), 24, 17, 9207-9210.
10. Holtz, J. H; Asher S. A. “Polymerized colloidal crystal hydrogel films as intelligent chemical sensing materials”, *Nature* (1997), 389, 829-832.
11. Jason, N. N.; Chaudhuri, R. G.; Paria, S. “Self-assembly of colloidal sulfur particles influenced by sodium oxalate salt on glass surface from evaporating drops”, *Soft Matter* (2012), 8, 3771-3780.
12. Kaya, D.; Belyi, V. A.; Muthukumara, M. “Pattern formation in drying droplets of polyelectrolyte and salt”, *J. Chem. Phys.* (2010), 133, 114905-1-8.
13. Kralchevskyt, P. A.; Nagayama, K. “Capillary Forces between Colloidal Particles”, *Langmuir* (1994), 10, 23-36 23.
14. Kundu, S.; Wang, K.; Liang, H. “Size-Controlled Synthesis and Self-Assembly of Silver Nanoparticles within a Minute Using Microwave Irradiation”, *J. Phys. Chem. C* (2009), 113, 134–141.
15. Lee, I.; Ahn, J. S.; Hendricks, T. R. “Patterned and Controlled Polyelectrolyte Fractal Growth and Aggregations”, *Langmuir* (2004), 20, 2478-2483.
16. Li, J.; Du, Q.; Sun, C. “An improved box-counting method for image fractal dimension estimation”, *Pattern Recognition* (2009), 42, 2460 – 2469.
17. Mullins, W. W.; Sekerka, R. F. “Morphological Stability of a Particle Growing by Diffusion or Heat Flow”, *J. Appl. Phys.* (1963), 34, 323-329.
18. Nagayama, K. “Two-dimensional self-assembly of colloids in thin liquid films”, *Colloids and Surfaces A* (1996), 109, 363-374.
19. Olgun U.; Sevinc. V. “Evaporation induced self-assembly of zeolite A micropatterns due to the stick–slip dynamics of contact line”, *Powder Technology* (2008), 183, 207–212.
20. Paunov, V. N.; Kralchevsky, P. A.; Denkov, N. D.; Nagakama, K. “Lateral Capillary Forces Between Submillimeter Particles”, *Colloid and Interfacial Science* (1993), 57, 100-112.
21. Prasada R. R.; Sreenivasan, K. R.” The measurement and interpretation of fractal dimensions of the scalar interface in turbulent flows” *J. Phys. Fluids A* (1990), 2, 5, 792-807.

22. Sharon, E.; Moore, M. G.; McCormick, W. D.; Swinney, H. L. “Coarsening of Fractal Viscous Fingering Patterns”, *Phys. Review Letters* (2003), 91, 20, 205504-1 – 205504-4.
23. Shukla, N.; Nigra, M. M. “Synthesis and self-assembly of magnetic nanoparticles”, *J. Surface Science* (2007), 601, 2615–2617.
24. Takhistov, P., Chang, H.-chiam “Complex Stain Morphologies”, *Ind. Eng. Chem. Res.* (2002), 41, 6256-6269.
25. Witten T. A.; Sander, L. M. “Diffusion-limited aggregation”, *Phys. Rev. B* (1983), 27, 9, 5686-5697.
26. Yamaki, M.; Higo, J.; Nagayama, K. “Size-Dependent Separation of Colloidal Particles In Two-Dimensional Convective Self-Assembly”, *Langmuir* (1995), 11, 2975-2978.
27. Yunker, P. J.; Still, T.; Lohr, M. A.; Yodh, A. G. “Suppression of the coffee-ring effect by shape-dependent capillary interactions”, *Nature* (2011), 476, 308-311.
28. Zhao, Q.; Qian, J.; Gui, Z.; An, Q.; Zhu, M. “Interfacial self-assembly of cellulose-based polyelectrolyte complexes: pattern formation of fractal trees”, *Soft Matter* (2010), 6, 1129-1137.
29. Zhao, Q.; An, Q.; Qian, J.; Wang, X.; Zhou, Y. “Insight into Fractal Self-Assembly of Poly (diallyldimethylammonium chloride)/Sodium Carboxymethyl Cellulose Polyelectrolyte Complex Nanoparticles”, *J. Phys. Chem. B* (2011), 115, 14901–14911.

